MOLECULAR AND CELLULAR BIOLOGY, Oct. 2005, p. 9103–9114 Vol. 25, No. 20
0270-7306/05/$08.00+0 doi:10.1128/MCB.25.20.9103–9114.2005

Regulation of Telomere Length by an N-Terminal Region of the Yeast Telomerase Reverse Transcriptase†

Hong Ji, Margaret H. Platts, Latif M. Dharamsi,‡ and Katherine L. Friedman*

Vanderbilt University, Department of Biological Sciences, VU Station B, Box 351634, Nashville, Tennessee 37235

Received 12 January 2005/Returned for modification 7 March 2005/Accepted 21 July 2005

Telomerase is a reverse transcriptase that maintains chromosome integrity through synthesis of repetitive telomeric sequences on the ends of eukaryotic chromosomes. In the yeast *Saccharomyces cerevisiae*, telomere length homeostasis is achieved through negative regulation of telomerase access to the chromosome terminus by telomere-bound Rap1 protein and its binding partners, Rif1p and Rif2p, and positive regulation by factors such as Ku70/80, Tel1p, and Cdc13p. Here we report the identification of mutations within an N-terminal region (region I) of the yeast telomerase catalytic subunit (Est2p) that cause telomere lengthening without altering measurable catalytic properties of the enzyme in vitro. These telomerase mutations affect telomere length through a Ku-independent mechanism and do not alter chromosome end structure. While Tel1p is required for expression of the telomere-lengthening phenotype, Rif1p and Rif2p are not, suggesting that telomere overextension is independent of Rap1p. Taken together, these data suggest that specific amino acids within region I of the catalytic subunit of yeast telomerase play a previously unanticipated role in the response to Tel1p regulation at the telomere.

Telomeres are nucleoprotein structures that cap the ends of linear eukaryotic chromosomes. In most species, these termini are composed of tandem, short G-rich repeats and associated protein complexes (reviewed in reference 56). Telomeres play an essential role in genome stability by preventing recognition of the normal chromosome terminus as a DNA double-strand break. However, the inability of the conventional DNA polymerase machinery to fully replicate terminal sequences results in gradual erosion of telomeric repeats, leading to checkpoint activation and cellular senescence. In cells that maintain proliferative potential, this end replication problem is counteracted by telomerase, a reverse transcriptase capable of synthesizing telomeric repeats onto chromosome ends using an intrinsic RNA template (18, 19). In budding yeast, *TLC1* and *EST2* encode the template RNA and reverse transcriptase subunit, respectively, of the catalytic core of the telomerase holoenzyme (27, 31, 50). As predicted, strains lacking these genes undergo progressive telomere shortening and senescence (referred to as the EST [*e*ver *s*horter *t*elomere] phenotype). Mutations of three additional genes (*EST1*, *EST3*, and *EST4* [*CDC13*]) result in the same phenotype (27, 34, 41). However, unlike strains lacking *EST2* or *TLC1*, strains bearing these mutations retain telomerase catalytic activity, suggesting that these proteins are essential regulators of telomere replication in vivo (30, 41).

Est2p belongs to a family of proteins (TERT; *te*lomerase *r*everse *t*ranscriptase) that contains a domain characteristic of reverse transcriptases in its C-terminal half (31). Sequence alignment among numerous TERT proteins as well as functional analysis in ciliate, yeast, and human TERT (1, 12, 13, 36, 38, 39, 59) have identified three additional essential regions (I, II, and III [12]; also called GQ, CP, and QFP [59] or RID1 and RID2 [39]) within the N-terminal half of the protein. Mutations within regions II and III of Est2p result in loss of coimmunoprecipitation with *TLC1* RNA (12, 29), suggesting that these regions participate in RNA binding. Similar sequences are required for association of ciliate and human TERT with their respective telomerase RNAs (4, 5, 24, 39).

TERT region I contributes several functions to the telomerase holoenzyme, many of which are incompletely understood. The RID1 domain of human telomerase (corresponding to *Saccharomyces cerevisiae* region I) interacts with the telomerase RNA and contributes to repeat addition processivity and multimerization (40). Mutations within a subset of these N-terminal residues of both yeast and human TERT (hTERT) abrogate telomere replication in vivo, while the catalytic activity of the enzyme is retained (1, 12). These residues define an N-terminal region of hTERT that *d*issociates *a*ctivities of *t*elomerase (N-DAT domain). A subset of N-DAT mutations are rescued by direct protein fusion of hTERT to telomere-binding proteins, suggesting that these residues contribute to the recruitment of telomerase to the telomere in vivo (2, 3).

Additional residues in the N-DAT domain have been implicated in primer association because substitution of these residues (amino acids 92 to 97) influences the primer preference of the holoenzyme in vitro (26). The existence of such a primer binding or anchor site in the telomerase enzyme has been inferred from a number of observations (7, 21, 25), including the propensity of yeast telomerase to remain tightly bound to its in vitro reaction products in a manner dependent on the 5′ end of telomeric primers (44). Because these 5′ nucleotides lie outside of sequences predicted to base pair with the telomerase RNA, this observation implies an interaction between the primer and protein component(s) of the complex. Indeed, a telomeric primer can be cross-linked to Est2p, supporting the

* Corresponding author. Mailing address: Vanderbilt University, VU Station B, Box 351634, Nashville, TN 37235. Phone: (615) 322-5143. Fax: (615) 343-6707. E-mail: katherine.friedman@vanderbilt.edu.

† Supplemental material for this article may be found at http://mcb.asm.org/.

‡ Present address: Emory University, Yerkes National Primate Research Center, 954 Gatewood Road NE, Atlanta, GA 30322.

TABLE 1. Strains used in this work

Strain	Genotype	Source or reference
TVL268	*MAT***a** *ura3-52 ade2-101 lys2-801 leu2-Δ1 trp1-Δ1 his3-Δ200* chromosome fragment [*TRP1 SUP11*]	V. Lundblad
YKF120-404	TVL268 *est2Δ::HIS3*/pKF404 *(EST2 URA3 CEN)*	This paper
YKF120-410	TVL268 *est2Δ::HIS3*/pKF410 (ProA-*EST2 URA3 CEN*)	This paper
YKF120-410^{LT}	TVL268 *est2Δ::HIS3*/pKF410-*est2*^{LT} *(*ProA-*est2*^{LT} *URA3 CEN)*[a]	This paper
YKF114-404	TVL268 *est2::HIS3 rad52::LEU2*/pKF404	This paper
YKF114-410	TVL268 *est2Δ::HIS3 rad52::LEU2*/pKF410	This paper
YKF114-E76K	TVL268 *est2Δ::HIS3 rad52::LEU2*/pKF410-*E76K (*ProA-*est2*^{E76K} *URA3 CEN)*	This paper
YKF201[b]	*MAT***a** *trp1 leu2 ura3 his7*	11
YKF201-α	*MATα trp1 leu2 ura3 his7*	This paper
YKF201-E76K	YKF201 *est2*^{E76K}	This paper
YKF202	YKF201 *tel1Δ::KAN*^{R}	This paper
YKF202-E76K	YKF202 *est2*^{E76K}	This paper
YKF203	YKF201 *yku70Δ::KAN*^{R}	This paper
YKF203-E76K	YKF203 *est2*^{E76K}	This paper
YKF204	YKF201 *rif1Δ::KAN*^{R}	This paper
YKF204-E76K	YKF204 *est2*^{E76K}	This paper
YKF205	YKF201 *rif2Δ::KAN*^{R}	This paper
YKF205-E76K	YKF204 *est2*^{E76K}	This paper
DKF206	*MAT***a**/*MATα trp1/trp1 leu2/leu2 ura3/ura3 his7/his7*	This paper
DKF207	*MAT***a**/*MATα trp1/trp1 leu2/leu2 ura3/ura3 his7/his7 est2*^{E76K}/*est2*^{E76K}	This paper
DKF208	*MAT***a**/*MATα trp1/trp1 leu2/leu2 ura3/ura3 his7/his7 EST2/est2*^{E76K}	This paper
BY4705a	*MAT***a** *ade2::hisG his3Δ200 leu2Δ0 lys2Δ0 met15Δ0 trp1Δ63 ura3Δ0 hdf1::LEU2*	R. Wellinger

[a] pKF410-*est2*^{LT} strains are variants of plasmid pKF410 expressing mutant *est2* alleles (*est2*^{G75A}, *est2*^{E76K}, *est2*^{N95A}, *est2*^{N95D}, and *est2*^{FCA720WCG}) as indicated in the text.

[b] This strain was previously named 4053-5-2.

hypothesis that the anchor site lies in region I of Est2p (32). Finally, overexpression of yeast *EST3* specifically suppresses temperature-sensitive mutations in *EST2* region I, suggesting that N-terminal residues of the yeast catalytic subunit may also play a role in recruiting the Est3 protein to the complex (13).

In most species, telomeric DNA is maintained at a constant average length by a dynamic process that involves a number of regulatory proteins in addition to telomerase. In *S. cerevisiae*, telomere length varies between 225 and 375 bp (reviewed in reference 60). This average telomere length is maintained by a balance between the telomere-lengthening activity of telomerase and negative regulation of telomerase by the double-stranded telomeric DNA binding protein Rap1p and its associated factors (22, 23, 28, 37, 58). Rap1p binds to the double-stranded telomeric repeats in yeast where it is thought to nucleate binding of a number of additional proteins to the telomere. As the number of bound Rap1 molecules increases, the accessibility or activity of telomerase at the telomere decreases, thereby allowing Rap1p to effectively "measure" telomere length (reviewed in reference 51). Recent results suggest that telomeres switch between telomerase-accessible and -inaccessible states and that Rap1p and its binding partners Rif1p and Rif2p are critical determinants of those states (54). Mutations in *RIF1* and *RIF2*, or C-terminal mutations in *RAP1* that prevent association of Rif1p and Rif2p with the telomere, result in telomere overelongation (22, 23, 58). Although the precise mechanism through which the binding of Rap1p affects telomerase activity is not understood, this negative regulation is dependent on the activity of the Tel1p kinase. Deletion of *TEL1* results in significant telomere shortening (35). Furthermore, deletion of *TEL1* in *rif1*Δ or *rif2*Δ strains or in a strain lacking the C terminus of Rap1p reduces telomere length to the same degree as *tel1*Δ alone (9, 45). Therefore, *TEL1* acts downstream of *RAP1*, *RIF1*, and *RIF2*.

In this paper, we identify several mutations clustered within region I of Est2p that result in overelongated telomeres (*est2*^{LT} alleles). Although the *est2*^{LT} alleles lie in a region of Est2p that corresponds to residues implicated in primer binding, we find no evidence of defects either in primer binding or catalysis by telomerase immunopurified from *est2*^{LT} strains. Genetic epistasis analysis suggests that these mutations lengthen telomeres by a Tel1p-dependent mechanism but are independent of Rif1p and Rif2p. We propose that these mutations in Est2p region I influence a previously unrecognized regulatory function of the catalytic subunit.

MATERIALS AND METHODS

***S. cerevisiae* strains and plasmids.** Strains utilized in this work are summarized in Table 1. The *est2*^{E76K} mutation and an overlapping HindIII restriction site were generated by PCR utilizing primers HindIIIR (5′ GTACGTTGTTGTA**A AGCTT**GCCCGTCAACAGG) and HindIIIF (5′ CCTGTTGACGGGC**AAGC TT**TACAACAACGTAC). Residues introducing the E76K mutation are bold, and the HindIII restriction site is underlined. pKF409-TVL268 (ProA-*EST2 URA3*; see reference 13) was the template. The mutagenized PCR product was cleaved with AflII and NheI and ligated to the corresponding sites of pKF409-TVL268. pKF408-E76K was created by cloning the AflII-NheI fragment of pKF409-E76K into pKF408 (untagged *EST2 URA3* [12]). The entire cloned fragment was sequenced.

pKF408-N95A AatII was created as described above using mutagenic primers 5′ CTGAAATGAA**GACGTC**GCAAATAGTCTTTTTTGC and 5′ GCAAAAA AGACTATT**TGC**GACGTCTTCATTTCTAGC (nucleotides introducing the N95A mutation are bold; the AatII restriction site is underlined). The resulting PCR product was cleaved with PflMI and AflII and ligated into the corresponding sites of pKF408 (*EST2 URA3*). The cloned fragment was fully sequenced.

A strain containing the *est2*^{E76K} allele integrated at the endogenous locus was created by cleaving pKF408-E76K with ClaI and transforming strain YKF201 (Table 1) by two-step gene replacement (48) to create strain YKF201-E76K.

Complete gene disruptions of *TEL1*, *YKU70*, *RIF1*, and *RIF2* were obtained by

amplifying the *KAN*^{R} gene and flanking DNA from the appropriate strain (15; Open Biosystems, Huntsville, AL). After transformation of the PCR product into YKF201 and YKF201-E76K, transformants were selected on yeast-peptone-dextrose media containing 200 μg/ml Geneticin. Successful knockout was confirmed by PCR and/or Southern blotting.

Homozygous diploid strains were obtained by transforming YKF201 and YKF201-E76K with pHO, a plasmid expressing the HO endonuclease (16). Transformants were restreaked twice, plated on 5-fluoroorotic acid to select for plasmid loss, and tested for diploidy. The heterozygous diploid strain (*EST2*/*est2*^{E76K}) was obtained by mating YKF201-E76K with YKF201α (obtained by sporulation of the *EST2*/*EST2* diploid described above).

Screen for long-telomere mutants. Construction of pKF410-*est2*^{N95A}, *est2*^{G75A}, and *est2*^{N95D} has been described previously (13). Additional alleles of *EST2* were created by a gap repair approach utilizing unique AflII and PflMI restriction sites located at amino acids 59 and 119 of Est2p, respectively. Primers JW75 (5′-GTTTCGCACTACCAAATTCAAG) and JW95 (5′-CTGCCCATTAAATTGAATTACTG) were used to amplify a 305-bp fragment by error-prone PCR as described previously (14). The resulting PCR product and pKF410 FS vector (linearized with AflII and PflMI) were cotransformed into strain YKF120 (Table 1; following loss of the complementing plasmid on 5-fluoroorotic acid). pKF410 FS was created by ligating an NheI-AflII fragment of pKF408-N95A AatII (see above) into the NheI-AflII sites of pKF410. The resulting plasmid was cleaved with AatII, treated with T4 DNA polymerase, and religated.

Ura$^+$ transformants obtained by gap repair were restreaked several times to eliminate mutants that inactivated *EST2*. DNA was isolated from transformants showing robust growth after the third restreak using either a DNA-Pure Yeast Genomic kit (CPG Inc.) or bead lysis (47), and telomere length was analyzed by Southern blotting as previously described (13) following cleavage with PstI or XhoI as indicated in the figure legends. Genomic DNA from strains showing longer-than-normal telomeres by Southern blotting was used to transform *Escherichia coli* by electroporation, and rescued plasmids were retested for effects on telomere length.

In-gel hybridization procedure. In-gel hybridization was done as described previously with some modifications (10; A. Bertuch, personal communication). A 22-mer (5′ CCCACCACACACACCCACACCC) was gel purified and labeled by incubation at 37°C for 45 min with [γ-^{32}P]ATP and T4 polynucleotide kinase (Roche). Yeast genomic DNA was isolated using bead lysis (47), and equivalent amounts of DNA were digested by XhoI in a 100-μl reaction volume. Reactions were terminated by precipitation with 20 μl 3 M NaOAc and 660 μl 100% ethanol. Pellets were resuspended in 12 μl binding buffer (10 mM Tris-HCl, 50 mM NaCl, 10 mM $MgCl_2$, 1 mM dithiothreitol [DTT], pH 7.9, at 25°C), 1 μl probe (100,000 cpm) was added to each sample, and samples were incubated for 10 min at 37°C, followed by incubation for 1 h on ice. Samples were loaded on Sephadex G-50 columns to eliminate unbound probe. DNA samples were separated in a 0.7% agarose gel by electrophoresis for 16 h at ~2 V/cm in a cold room. Gels were dried at 23°C (using a SGD5040 slab gel dryer; Savant) for 24 to 28 min until the gel was very thin and even, and the gel was exposed to phosphorimager screen.

To denature the chromosomal DNA, the gel was washed in denaturing solution (0.15 M NaCl, 0.5 M NaOH) for 25 min at room temperature, followed by a 25-min wash in neutralizing solution (0.15 M NaCl, 0.5 M Tris HCl, pH 8.0). The gel was briefly prehybridized with 25 ml hybridization solution (8), and 18 μl of the probe described above was added. The gel was incubated at 36°C overnight. The gel was washed in 0.25× SSC (1× SSC is 0.15 M NaCl plus 0.015 M sodium citrate) at room temperature overnight and exposed to phosphorimager screen.

Primer competition assay. Extract preparation and immunoprecipitation of protein A-tagged Est2p was performed as described previously (19), except that beads were washed two times with TMG (10 mM Tris-Cl at pH 8, 1 mM $MgCl_2$, 10% glycerol, 0.1 mM DTT) plus 200 mM NaCl and 0.5% Tween 20 and twice with TMG plus 2 μl/ml RNasin (Promega) and were resuspended in 20 μl of TMG (plus 2 μl/ml RNasin, 0.5 mM DTT). Prior to immunoprecipitation, extract concentrations were adjusted to 20 mg/ml. Packed beads (5 μl) from the immunoprecipitation were mixed with 0.5 μl of water or 0.5 μl of 1 mg/ml RNase A and incubated for 10 min at 30°C. A 2× reaction mixture (5.5 μl) consisting of 80 mM Tris-Cl at pH 8, 100 mM NaCl, 10% glycerol, 5 mM $MgCl_2$, 1 mM spermidine, 1 mM DTT, 5 μM initial substrate oligonucleotide (see below), 200 μM each dTTP, dATP, and dCTP, and 1.5 μl [α-^{32}P]dGTP (800 Ci/mM; 10 μCi/μl) was added per sample on ice, and the reaction was initiated by incubation at 30°C. After 7 min, 1.4 μl of 20 μM challenge oligonucleotide (or 1.5 μl buffer) was added, and the incubation was continued for an additional 23 min. The reaction was stopped by addition of 1.5 μl of stop buffer (250 mM Tris at pH 8, 250 mM EDTA at pH 8, 2% sodium dodecyl sulfate) and 1.75 μl of proteinase K (20 mg/ml) for 30 min at 60°C. Reaction products were phenol extracted, precipitated, and separated in a 12% acrylamide/8 M urea sequencing gel. Product was quantitated after exposure to a phosphorimager. Oligonucleotide +1 marker was made by treating the appropriate oligonucleotide with terminal transferase (GE Healthcare) in the presence of [^{33}P]ddTTP. Substrate (and challenge) oligonucleotides were as described previously (44): 14 (5′ GTGTGGTGTGTGGG); 5′NT (5′ GACCGCGGTGTGTGGG); and 29 (5′ GGGTGTGGTGTGTGGGTGTGGTGTGTGGG).

Nucleotide addition processivity. Extract preparation and immunoprecipitation were as described above. To visualize differences in processivity between wild-type and *est2*^{FCA720WCG} strains, the conditions of the telomerase assay were modified as described previously (42). Reactions were incubated at room temperature for 1 h, then processed as described above. Reaction products were quantified by determining the intensity of each band (+1 to +7) by phosphorimager analysis. Processivity^{+3} was calculated as the sum of signal in bands +4 to +7 divided by the total amount of signal in bands +1 to +7. Signal was corrected for specific activity by dividing the intensity of each position by the number of G residues expected to be incorporated into the product at that position (+2, +3 = 1; +4 = 2; +5, +6 = 3; +7 = 4).

Analysis of primer binding. Extract preparation, immunoprecipitation, and the telomerase assay were done essentially as described above for the primer competition assay with the following adjustments. All deoxynucleoside triphosphates were omitted and [α-^{32}P]dTTP (800 Ci/mM; 10 μCi/μl) was substituted for dGTP. Primer was added to immunopurified telomerase at 5× decreasing final concentrations of 2.5 μM, 0.50 μM, 0.10 μM, 0.02 μM, 0.004 μM, and 0.0008 μM for 10 min on ice. Reactions were initiated by the addition of telomerase reaction mix containing dTTP and allowed to proceed for 7 min at 30°C before being terminated by the addition of stop buffer and proteinase K as described above. Equal amounts of an end-labeled 29-mer oligonucleotide was added to each sample prior to phenol extraction and precipitation to serve as a loading control. Reaction products were quantified by using a phosphorimager. The intensity of each +1 product band (corrected for background) was divided by the intensity of the loading control to correct for variations in yield during sample processing. The corrected value for the +1 product was then normalized to that of the highest primer concentration to correct for variations between experiments in specific activity of the loading control.

Western blotting. Protein extraction and immunoprecipitation with immunoglobulin G (IgG) Sepharose beads (GE Healthcare) were performed as previously described (12). Samples were loaded on a NuPAGE 10% Bis-Tris gel (Invitrogen). Protein was transferred to a Hybond-P membrane (GE Healthcare). Primary antibody was mouse monoclonal anti-protein A (Sigma). Secondary was peroxidase-conjugated goat anti-mouse antibody (Chemicon International).

RESULTS

Identification of mutations in *S. cerevisiae EST2* that increase telomere length. In the course of analyzing telomere length in a large number of strains containing mutations within the N-terminal half of Est2p, we fortuitously identified three mutations (glycine 75 to alanine [G75A] and asparagine 95 to alanine or aspartic acid [N95A, N95D]; Fig. 1A) that resulted in telomere overelongation (Fig. 1B, compare lanes 2 and 3, lanes 5 and 6, and lanes 11 and 12 with lanes 1, 4, 7, and 10). Of the 800-bp telomeric fragment derived from PstI digestion in the subtelomeric Y′ element (Fig. 1B, line), approximately 250 to 350 bp comprise telomeric repeat sequences. In this strain background, G75A increased the average length of the terminal PstI fragment by approximately 30 bp, while N95A and N95D caused a 50-bp increase (20%). Twenty-five other mutations in conserved and nonconserved residues of the N-terminal half of *EST2* caused telomeres to be maintained at normal or shorter-than-normal length (data not shown; 13).

Because of the clustering of the *est2*^{LT} alleles in the primary amino acid sequence of Est2p, we screened within a 60-amino-acid region encompassing *EST2* amino acids 59 to 119 for additional mutations resulting in this phenotype. Briefly, a plasmid encoding protein A-tagged *EST2* (ProA-*EST2*) was

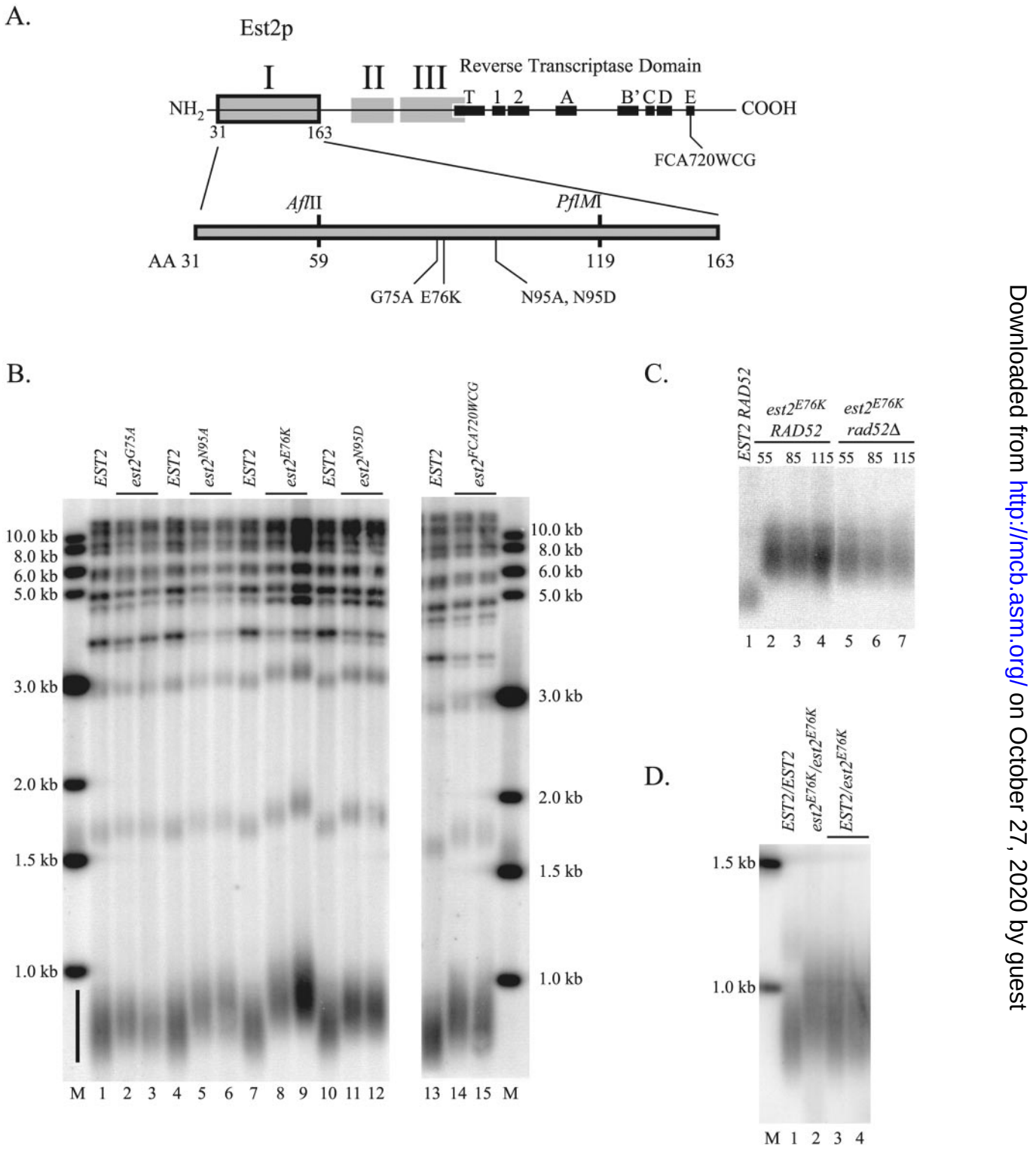

FIG. 1. Mutations in region I of Est2p cause telomere lengthening. (A) Map of functional regions of Est2p. Top: map of Est2p primary sequence indicating the locations of the reverse transcriptase domain and three N-terminal regions that are essential for telomere maintenance in yeast. The location of the *est2*^{FCA720WCG} mutation is indicated (42). Bottom: detailed map of region I of Est2p. The locations of mutations that result in telomere lengthening are indicated (G75A, glycine 75 to alanine; E76K, glutamic acid 76 to lysine; N95A, asparagine 95 to alanine; N95D, asparagine 95 to aspartic acid). Unique AflII and PflMI restriction sites were used in a gap repair strategy to identify additional alleles of *est2* with the long-telomere phenotype (see text). (B) Telomere length is increased in strains expressing plasmid-borne *est2*^{LT} alleles. All strains are derived from YKF120 (*est2*::*HIS3*) and carry plasmids expressing wild-type or mutant protein A-tagged *EST2*. Genomic DNA from strains expressing ProA-*EST2* (lanes 1, 4, 7, 10, and 13), ProA-*est2*^{G75A} (lanes 2 and 3), ProA-*est2*^{N95A} (lanes 5 and 6), ProA-*est2*^{E76K} (lanes 8 and 9), ProA-*est2*^{N95D} (lanes 11 and 12), or ProA-*est2*^{FCA720WCG} (lanes 14 and 15) was digested with PstI, separated in a 1.2% agarose gel, blotted, and probed with

cleaved with PflMI and AflII (Fig. 1A), and the resulting gapped vector DNA was cotransformed into an *est2*::*HIS3* yeast strain with an overlapping PCR product generated under mutagenic conditions (see Materials and Methods). Transformants recovered on media lacking uracil were restreaked three times (eliminating any senescent colonies bearing nonfunctional *EST2*), and the resulting healthy strains were screened for increased telomere length by Southern blotting. Of ~700 colonies screened, four caused increased telomere length upon plasmid isolation and reintroduction. All four plasmids contained a mutation of glutamic acid 76 to lysine (E76K). Although several of these plasmids contained mutations in addition to E76K, subcloning revealed that the long-telomere phenotype was exclusively due in each case to the E76K mutation (data not shown). In this strain, the E76K mutation increased average telomere length by about 100 bp (40%; Fig. 1B, lanes 8 and 9).

A mutation within motif E of the reverse transcriptase motif of *EST2* (*est2*^{FCA720WCG}; Fig. 1A) was previously reported to cause telomere lengthening equivalent to that described here (42). Indeed, when this mutation was incorporated into a plasmid-borne, protein A-tagged allele of *EST2* and transformed into our *est2*::*HIS3* strain, the extent of telomere lengthening was similar to that caused by the *est2*^{N95A} and *est2*^{G75A} mutations (Fig. 1B, lanes 14 and 15).

Because the ProA-*EST2* allele causes slightly decreased telomere length (~50 bp), we were concerned that the effect of telomere lengthening by the *est2*^{LT} alleles might result from stabilization specific to the protein A-tagged protein. To address this possibility, *est2*^{E76K} was introduced into the chromosome at the endogenous locus (in the absence of the protein A tag) and telomere length was assayed by Southern blotting. Under these conditions, the increase in telomere length was comparable to that seen with the plasmid-borne, tagged allele (data not shown; see also Fig. 7A, lanes 1 and 2), confirming that the mutation does not simply counteract the negative effect of the epitope tag.

In the absence of functional telomerase, most cells die after ~75 generations. However survivors arise that maintain heterogeneous telomeres through Rad52p-mediated recombination (33). To assess the role of recombination in telomere lengthening, a plasmid bearing the *est2*^{E76K} allele was introduced into an *est2*Δ *rad52*Δ strain, and the resulting transformants were grown for ~115 generations in liquid culture. Telomere lengthening was identical to that seen in an *est2*Δ *RAD52* background (Fig. 1C, compare lanes 2 to 4 with lanes 5 to 7). Therefore, recombination does not contribute to the long-telomere phenotype. This result also demonstrates that the mutants reach a new, stable telomere length equilibrium and do not undergo continuous elongation.

We considered the possibility that the *est2*^{E76K} allele alters the interaction of Est2p with one or more components of the telomerase complex. Coimmunoprecipitation experiments demonstrated that the ability of the ProA-Est2^{E76K} protein to bind HA-Est1p, HA-Est3p, and Myc-PinXIp was equivalent to that of the wild type (see Fig. S1 in the supplemental material), arguing that alteration of the relative stoichiometry of these components in the telomerase complex does not contribute to the telomere-lengthening phenotype.

To address whether the telomere-lengthening phenotype conferred by *est2*^{E76K} is dominant or recessive to the wild type, we created a heterozygous diploid strain. As shown in Fig. 1D, two independent *EST2*/*est2*^{E76K} diploid strains (lanes 3 and 4) had telomere lengths intermediate between those of an *EST2*/*EST2* diploid (lane 1) and an *est2*^{E76K}/est2^{E76K} diploid (lane 2). The telomere length of the heterozygous diploid strain was more heterogeneous than either homozygous diploid strain. We conclude that the *est2*^{E76K} allele is semidominant.

Nucleotide addition processivity of *est2*^{LT} alleles is normal. The similarity in telomere phenotype between the *est2*^{LT} region I mutants and the *est2*^{FCA720WCG} mutant (Fig. 1B) suggested that these alleles might be mechanistically related. Increased nucleotide addition (type I) processivity demonstrated by the *est2*^{FCA720WCG} allele in vitro has been hypothesized to account for increased telomere length in vivo (42). To address whether the *est2*^{LT} mutations also increase type I processivity, telomerase was partially purified from yeast cells expressing protein A-tagged Est2p by adsorption to IgG beads. Bead-bound telomerase was incubated in the presence of [^{32}P]dGTP, cold dTTP, and a 14-nucleotide telomeric primer. This oligonucleotide primer aligns with the telomerase RNA to allow addition of up to seven nucleotides in a single round of polymerization (Fig. 2A). Because yeast telomerase remains bound to its reaction products under these conditions (44), the enzyme does not demonstrate repeat addition (type II) processivity—the ability to add multiple repeats to a single primer. Indeed, because most primers fail to become extended to the end of the template, a ladder of products (+2 to +7) is visualized even after prolonged incubation (Fig. 2B). Because the largest effect on processivity was previously shown to occur at the third template position (42), nucleotide addition processivity was expressed as a processivity$^{(+3)}$ value (probability that the enzyme extends past the $n + 3$ position; [42]) by summing the intensity of the last four template positions ($n + 4$ to $n +$

telomeric DNA. The black bar indicates a smear of fragments derived from the 2/3 of yeast chromosomes that contain a subtelomeric Y′ element. Upper bands derive from non-Y′ telomeres and tandemly repeated Y′ elements. The sizes of marker bands (M) are indicated. (C) Telomere lengthening caused by *est2*^{E76K} is stable and independent of Rad52p. Strains YKF120 (*est2*::*HIS3 RAD52*; lanes 2 to 4) and YKF114 (*est2*::*HIS3 rad52*::*LEU2*; lanes 5 to 7) were transformed with pKF410-*est2*^{E76K}, a low-copy-number vector expressing the ProA-tagged *est2*^{E76K} allele. Transformants were restreaked once on media lacking uracil, and a single colony was grown to saturation in 5 ml liquid media lacking uracil. Liquid cultures were serially diluted 1,000-fold and allowed to regrow to saturation a total of 10 times. Genomic DNA was harvested from samples corresponding to approximately 55 (lanes 2 and 5), 85 (lanes 3 and 6), and 115 generations (lanes 4 and 7) after transformation of the mutant allele, digested with PstI, separated by gel electrophoresis, and probed with a telomeric probe. The control lane contains DNA harvested from YKF120 (*est2*::*HIS3 RAD52*; lane 1) transformed with a plasmid expressing protein A-tagged wild-type *EST2* (pKF410) and grown for a minimum of 115 generations. Only the telomeric smear corresponding to Y′ chromosomes is shown. (D) The *est2*^{E76K} allele is semidominant to the wild type. DNA from diploid strains *EST2*/*EST2* (DKF206; lane 1), *est2*^{E76K}/*est2*^{E76K} (DKF207; lane 2), and *EST2*/*est2*^{E76K} (DKF208; lanes 3 and 4) was digested with PstI and subjected to Southern blotting as described above. The sizes of marker bands are indicated (M).

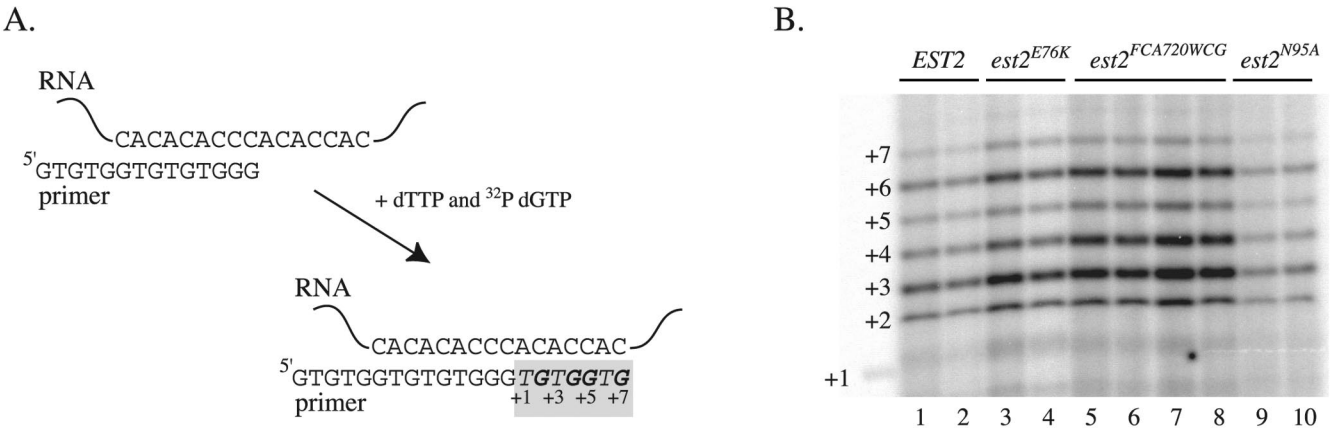

FIG. 2. Processivity of telomerase is increased by a mutation in motif E but not by mutations in the N-terminal region. (A) Schematic diagram of the in vitro telomerase assay. Extension of a 14-nucleotide telomeric primer by immunopurified telomerase in the presence of dTTP and radiolabeled dGTP results in the addition of up to seven nucleotides. (B) Primer extension of the 14-nucleotide primer by wild-type or mutant telomerase. Extract was isolated from strain YKF120 (*est2*::*HIS3*) bearing plasmids expressing the indicated *EST2* alleles (ProA-*EST2*, lanes 1 and 2; ProA-*est2*^{E76K}, lanes 3 and 4; ProA-*est2*^{FCA720WCG}, lanes 5 to 8; ProA-*est2*^{N95A}, lanes 9 and 10), and telomerase was immunopurified on IgG beads. Telomerase assays were performed as described in Materials and Methods. The positions of each consecutive nucleotide added to the 14-nucleotide primer are indicated. +1 marks the position of a 14 + 1 marker created by incubation of the 14-nucleotide primer with ^{32}P-labeled ddTTP and terminal transferase. Processivity of the wild-type and mutant telomerase was calculated from this and other similar experiments (data not shown) as summarized in Table 2.

7) and dividing by the total intensity at all seven template positions (corrected for specific activity; see Materials and Methods). As expected, the *est2*^{FCA720WCG} allele showed a significant increase in type I processivity at the third template position (Fig. 2B; Table 2). The percent change in processivity compared to wild type (31% increase) was comparable to that previously reported (42), although the absolute processivity value for wild-type telomerase was lower in our experiments. In contrast to *est2*^{FCA720WCG}, the *est2*^{N95A} and *est2*^{E76K} alleles had processivity$^{(+3)}$ values indistinguishable from those of the wild type (Fig. 2B; Table 2). We conclude that the telomere length increase caused by mutations in the N-terminal domain of *EST2* differs mechanistically from that resulting from a mutation in motif E of the reverse transcriptase domain.

Primer binding of *est2*^{LT} alleles is unaffected. Recent results suggest that the yeast anchor site lies within region I of Est2p (32). Because altered primer binding might cause telomere lengthening, we addressed the ability of the *est2*^{LT} alleles to bind telomeric primer using two independent assays. The first was a primer competition experiment described by Prescott and Blackburn (44). Because yeast telomerase displays single turnover kinetics in vitro, a challenge primer added several minutes after the initiation of primer extension is not utilized. This property is hypothesized to arise from persistent interactions between the telomerase holoenzyme and its reaction products, perhaps mediated by the anchor site. Indeed, a primer with nontelomeric sequence at its 5′ end (5′NT primer) is extended normally by telomerase in vitro but fails to block the use of the challenge primer (44). We reasoned that a mutation in the telomerase enzyme itself (perhaps in Est2p) that reduces primer interaction might similarly increase extension of the challenge primer in this assay. Both wild-type and mutant telomerase were immunopurified from whole-cell yeast extract and subjected to incubation with one primer, followed by addition of the challenge primer. In agreement with previous results (44), the challenge primer showed minimal extension in reactions with the wild-type enzyme, regardless of the order of addition of the differing length primers (Fig. 3, lanes 2 to 5, 8, and 9). However, clear extension of the challenge primer was detected in combination with the 5′NT primer (Fig. 3, lanes 6 and 7 and lane 10). Identical results were obtained with extract derived from cells expressing *est2*^{E76K}, *est2*^{G75A}, *est2*^{N95A}, and *est2*^{FCA720WCG} (Fig. 3, lanes 11 to 13; also data not shown). The ratio with which the 5′NT and long primers were utilized was indistinguishable for wild-type and *est2*^{E76K} telomerase, suggesting that this mutation does not confer a defect in primer binding as measured in this assay. Furthermore, because these assays were conducted in the presence of all four nucleotides, the failure to detect products longer than +7 (Fig. 3) indicated that the *est2*^{LT} alleles do not cause extension past the template boundary.

We were concerned that increased primer binding would not be detected in the primer competition assay. Therefore, we also examined the response of wild-type and mutant enzymes

TABLE 2. Processivity values of *est2*^{LT} alleles

Strain	Processivity$^{(+3)a}$ (*n*)	% Change^b	Significance^c
EST2	0.228 ± 0.009 (6)		
est2^{FCA720WCG}	0.298 ± 0.007 (4)	+31	$P \leq 0.002$
est2^{N95A}	0.229 ± 0.005 (4)	+0.4	$P \leq 0.91$
est2^{E76K}	0.216 ± 0.030 (4)	−5.0	$P \leq 0.38$

[a] Processivity$^{(+3)}$ refers to the frequency with which telomerase synthesizes past the third position. See Materials and Methods for details of calculation. Standard deviation (±) is indicated as well as the number of independent samples (in parentheses).

[b] Percent change of processivity$^{(+3)}$ from wild type is calculated using the average values shown in the second column.

[c] Significance values were determined relative to wild type using a Student *t* test.

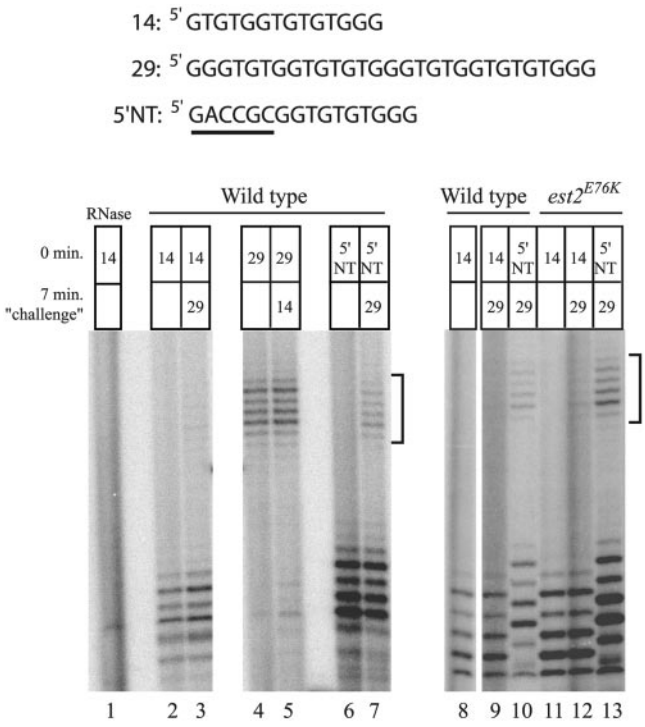

FIG. 3. Yeast telomerase containing a mutation at Est2p residue E76 does not exhibit a detectable decrease in product association in a primer competition assay. Extract was isolated from strain YKF120 (*est2*::*HIS3*) containing plasmids expressing either wild-type, protein A-tagged *EST2* (ProA-*EST2*, lanes 1 to 10) or protein A-tagged *est2*^{E76K} (ProA-*est2*^{E76K}, lanes 11 to 13), and telomerase was immunopurified on IgG beads. Primer sequences are shown (top). Primers 14 and 29 contain the canonical telomeric sequence, while primer 5′NT contains nontelomeric sequence at its 5′ end (underlined). Telomerase assays were performed using the indicated combinations of primers (see boxes). The top primer was added at the beginning of the reaction, while the bottom primer (or buffer alone; empty box) was added after the reaction had proceeded for 7 min. Products resulting from extension of the 29-nucleotide primer are indicated with brackets. Lane 1 contains a sample that was pretreated with RNase A to eliminate telomerase activity.

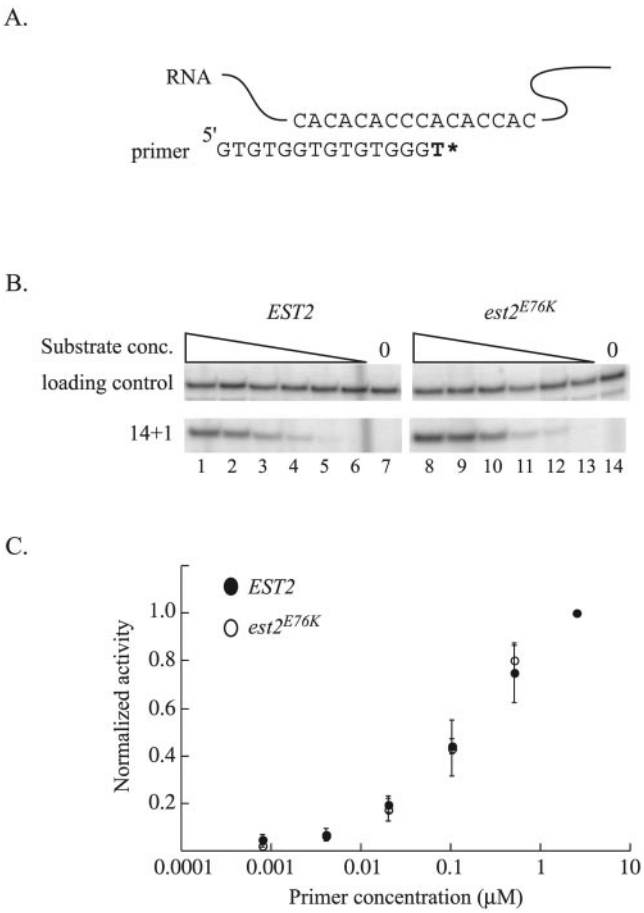

FIG. 4. The ability of telomerase to bind primer is unchanged by mutation of Est2p residue E76. (A) Schematic diagram of the in vitro telomerase assay. Extension of a 14-nucleotide telomeric primer by immunopurified telomerase in the presence of radiolabeled TTP alone results in the addition of a single nucleotide. (B) Change in activity of wild-type and mutant telomerase with decreasing primer concentrations. Telomerase was partially purified from strain YKF120 (*est2*::*HIS3*) containing plasmids expressing either wild-type, protein A-tagged *EST2* (ProA-*EST2*, lanes 1 to 7) or protein A-tagged *est2*^{E76K} (ProA-*est2*^{E76K}, lanes 8 to 14) by incubation with IgG-conjugated beads. Standard telomerase assays were conducted (see Materials and Methods) at decreasing primer concentrations. Production of the 14 + 1 product and recovery of a labeled 29-nucleotide precipitation and loading control is shown. Primer concentrations are 2.5 μM (lanes 1 and 8), 0.50 μM (lanes 2 and 9), 0.10 μM (lanes 3 and 10), 0.02 μM (lanes 4 and 11), 0.004 μM (lanes 5 and 12), and 0.0008 μM (lanes 6 and 13). Lanes 7 and 14 are assays done in the absence of primer. (C) Quantification of telomerase activity in response to decreasing primer concentrations. Band intensities in the experiment shown in Fig. 5B and others (data not shown) were determined by a phosphorimager. After adjustment for loading and precipitation efficiency, values were normalized to activity obtained at the highest primer concentration (see Materials and Methods for detail). Primer concentration (log axis) is graphed versus average, normalized activity level. Error bars represent standard deviations calculated from three independent experiments for the wild type and two independent experiments for *est2*^{E76K}.

to decreasing primer concentrations. Telomerase immunopurified from *EST2* and *est2*^{E76K} strains was incubated with 5× serial dilutions of a telomeric 14-mer primer and [^{32}P]dTTP. In the absence of dGTP, telomerase adds only a single nucleotide to the telomeric primer (Fig. 4A). The amount of primer extension product formed at each time point was quantified and normalized using a labeled, 28-nucleotide precipitation and loading control. Wild-type and *est2*^{E76K} telomerase were indistinguishable in this assay (Fig. 4B and C), showing that the apparent K_m for primer in the reaction is not affected by the *est2*^{E76K} allele.

We consistently observed a slight (less than twofold) increase in activity in Est2p immunoprecipitates from the *est2*^{E76K} strain (e.g., Fig. 2, compare lanes 1 and 2 with lanes 3 and 4). This increased activity can be attributed to a modest increase in the amount of Est2p immunoprecipitated from the mutant strain (Fig. 5A). However, when ProA-Est2p was detected in extract, expression of the wild-type and Est2^{E76K} proteins was equivalent (Fig. 5B). We conclude that the slightly elevated in vitro activity of the mutant protein reflects an increased efficiency of immunoprecipitation, rather than increased enzyme activity per se. Although we cannot rule out the contribution of subtle changes in enzyme activity, the re-

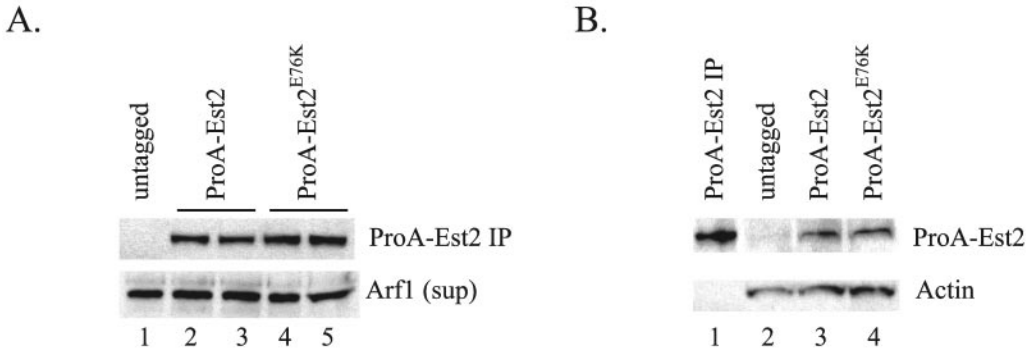

FIG. 5. Protein expression of wild-type and mutant Est2p is equivalent. (A) Immunoprecipitation of ProA-Est2p from extract. ProA-Est2p was immunoprecipitated (IP) on IgG-conjugated beads from strain YKF120 (*est2*::*HIS3*) containing plasmids expressing either untagged *EST2* (pKF404, lane 1), protein A-tagged *EST2* (pKF410, lanes 2 and 3), or protein A-tagged *est2*^{E76K} (pKF410-Est2^{E76K}, lanes 3 and 4) and detected by Western blotting using an anti-protein A primary antibody (top band). Duplicate lanes (2 and 3; 4 and 5) represent two independent immunoprecipitations from the same extract preparation to show reproducibility. Supernatants (sup) from the immunoprecipitations were Western blotted for the presence of Arf1p to verify equivalent extract concentrations (bottom band). (B) Detection of ProA-Est2p in extract. Extracts from strain YKF120 (*est2*::*HIS3*) containing plasmids expressing either untagged *EST2* (pKF404, lane 2), protein A-tagged *EST2* (pKF410, lane 3), or protein A-tagged *est2*^{E76K} (pKF410-Est2^{E76K}, lane 4) were Western blotted and probed with an anti-protein A primary antibody (top band). Lane 1 contains immunoprecipitated ProA-Est2p (identical to panel A, lane 2) as a size marker. Actin was detected as a loading control (bottom band).

sults presented here suggest that the *est2*^{LT} alleles do not alter the intrinsic catalytic properties of yeast telomerase.

The *est2*^{LT} alleles do not affect the single-stranded character of the telomere. To explore the possibility that the *est2*^{LT} alleles alter telomerase function in vivo, we used nondenaturing gel electrophoresis to probe the chromosomal end-structure in wild-type and mutant strains. In wild-type cells, yeast chromosomes acquire a long TG_{1-3} tail (more than 30 bp) late in S phase while the 3′ single-strand overhang is <15 bp during the remainder of the cell cycle (57). As a result, DNA isolated from asynchronous wild-type cells results in very little telomeric signal when cleaved with XhoI to release a terminal fragment of 1.3 kb and hybridized under nondenaturing conditions to an oligonucleotide that specifically recognizes the G-rich, telomeric 3′ overhang (Fig. 6A, lane 1). In contrast, a *ku70*Δ strain has long single-stranded telomeric overhangs that persist throughout the cell cycle and are therefore easily detected in asynchronous cells (Fig. 6A, lane 3; see reference 17). Hybridization in the native gel was specific to single-stranded DNA because treatment of the DNA with exonuclease I (ExoI) prior to hybridization eliminated the signal (Fig. 6A, even-numbered lanes).

Strains expressing the *est2*^{N95A}, *est2*^{E76K}, and *est2*^{FCA720WCG} alleles lacked telomeric signal in the native gel (Fig. 6A, lanes 5, 7, and 9, respectively), indicating no increase in single-stranded character compared to the wild-type strain (Fig. 6A, lane 1). The identical gel shown in Fig. 6A was denatured and rehybridized with the telomeric oligonucleotide to confirm equivalent loading of the samples (Fig. 6B). We conclude that the *est2*^{LT} alleles (and *est2*^{FCA720WCG}) do not significantly compromise replication or processing of the C-rich strand of the telomere.

The *est2*^{LT} alleles increase telomere length by a *TEL1*-dependent mechanism but are independent of *YKU70*, *RIF1*, and *RIF2*. To determine the genetic pathway through which the *est2*^{LT} alleles cause telomere lengthening, we used epistasis analysis to examine the involvement of several genes known to influence telomere length. The Ku70/80 complex and Tel1p act in different pathways to positively regulate telomere length (43). Therefore, we examined the effect of creating double mutations of these genes with the *est2*^{E76K} allele.

A deletion of *yku70* was introduced into strains expressing *EST2* or *est2*^{E76K}. Telomere length was assayed by Southern blotting after cleavage with PstI. As shown in Fig. 7A (lanes 3 and 4), the double mutant strain had a telomere length intermediate between those of the *yku70* deletion alone (lane 5) and the *est2*^{E76K} single mutant (lane 2). Restreaking of the double mutant strain nine times did not result in any further change in telomere length (Fig. 7A, compare lanes 3 and 4). Because the telomere-lengthening phenotype of the *est2*^{E76K} allele was expressed in the absence of Ku70p, we conclude that positive regulation by the Ku70/80 complex contributes little, if at all, to the *est2*^{LT} phenotype.

To test the requirement for Tel1p, a *tel1*::*kanMX* disruption was introduced into strains expressing *EST2* or *est2*^{E76K}. Two independent *est2*^{E76K} *tel1*Δ strains had telomeres intermediate in length compared with either single mutant when telomere length was assayed immediately after *TEL1* disruption (Fig. 7B, lanes 3 and 11, restreak 1). However, further propagation of the double mutant strains (to restreak 5) resulted in gradual telomere erosion until the double mutant strain attained a telomere length nearly as short as that of the *tel1*Δ strain (Fig. 7B, compare lanes 5 and 13 with lanes 9 and 17). Strikingly, both transformants displayed increased heterogeneity of telomere length after further restreaking (Fig. 7B, lanes 6 to 8 and 14 to 16). In this strain background, the *est2*^{E76K} mutation caused telomere length to increase by nearly 200 bp compared to wild type. In comparison, the *tel1*Δ *est2*^{E76K} strain displayed a telomere length at restreak 5 that was only 30 bp longer than the *tel1*Δ strain. We obtained identical results in a *tel1*Δ *est2*^{N95A} strain (data not shown). We conclude that telomere lengthening caused by the *est2*^{E76K} allele is nearly completely dependent on Tel1p, though there may be a minor contribution by a Tel1p-independent pathway.

Tel1p acts downstream of Rap1p in the regulation of telomere length (9). Therefore, it was possible that telomere

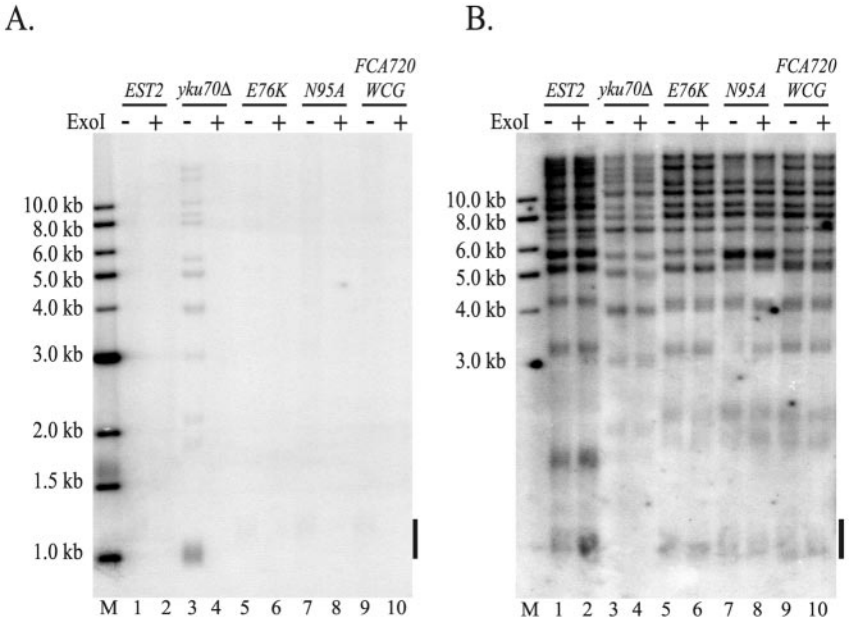

FIG. 6. The 3′ single-stranded overhang of *est2*^{LT} mutants is normal. (A) Single-stranded telomeric DNA detected by nondenaturing gel electrophoresis. All strains are derived from YKF120 (*est2*::*HIS3*) and carry plasmids expressing wild-type or mutant protein A-tagged *EST2*. Genomic DNA from strains expressing ProA-*EST2* (lanes 1 and 2), ProA-*est2*^{E76K} (lanes 5 and 6), ProA-*est2*^{N95A} (lanes 7 and 8), or ProA-*est2*^{FCA720WCG} (lanes 9 and 10) was digested with XhoI, incubated with a labeled 22-nucleotide telomeric probe, and subjected to nondenaturing gel electrophoresis. DNA from a *ku70* deletion strain previously demonstrated to increase the 3′ telomeric overhang (17) was used as a positive control (lanes 3 and 4). Samples in lanes 2, 4, 6, 8, and 10 were treated with exonuclease I prior to XhoI cleavage to remove the 3′ single-stranded overhang. The bar indicates the approximate position of the terminal XhoI fragment generated from chromosomes that contain a subtelomeric Y′ element. Additional bands detected in lane 3 correspond to individual telomeres lacking the Y′ element. Lane M, end-labeled DNA size standards. (B) Total telomeric DNA detected by hybridization after denaturation. The same gel shown in panel A was denatured by treatment with 0.5 M NaOH and hybridized with the telomeric probe described in panel A. The bar indicates the approximate position of the terminal XhoI fragment generated from chromosomes that contain a subtelomeric Y′ element. Although fragments corresponding to the shortest telomeres of the *yku70*Δ strain were preferentially lost during the wash steps, relative loading can be assessed by comparison of the higher-molecular-weight bands.

lengthening in the *est2*^{LT} strains occurred through the same genetic pathway as *RAP1*. Rif1p and Rif2p interact with the C terminus of Rap1 and negatively regulate telomere length (22, 58). As shown in Fig. 7C, *rif1*Δ and *rif2*Δ strains exhibit increased telomere length compared to a wild-type strain (compare lanes 3 and 5 with lane 1). When the *est2*^{E76K} mutation is combined with a *rif1* or *rif2* deletion, telomere length undergoes an additional increase in each case (Fig. 7C, lanes 4 and 6). We obtained identical results when double mutants were constructed using the *est2*^{N95A} allele (data not shown). We conclude that the telomere-lengthening phenotype of the *est2*^{LT} alleles is independent of *RIF1* and *RIF2*.

DISCUSSION

Telomere length homeostasis is critical to the maintenance of stable chromosomes. Previous work has suggested that telomere length is negatively regulated by protein factors that bind to telomeric chromatin (reviewed in reference 51). Specifically, Rap1p and its associated proteins bind to the telomeric repeat and regulate a molecular switch between telomerase-extendible and -nonextendible states (54). This mechanism of telomere length regulation is highly dependent on the chromatin context of the telomere, with telomerase presumably acting as a passive downstream target of the regulatory pathway. Here we show that mutations in a small region of the catalytic subunit of telomerase also cause telomere lengthening. Within the limits of our biochemical assays, the catalytic activity of the mutant enzyme is unaffected, indicating that the catalytic subunit of telomerase may play a previously unanticipated role in the regulation of telomerase activity at the telomere in vivo.

Catalytic activity of the mutant telomerase complex. The observation that telomeres become overelongated in the *est2*^{LT} strains initially suggested that telomerase in these strains may have increased or modified catalytic activity. Several observations argue against this possibility. Processivity of the enzyme is not altered, a phenotype that has previously been associated with telomere lengthening (42). Telomere lengthening by a defective telomerase enzyme might occur through infidelity of the enzyme resulting in abnormal repeat sequences. Such sequences might disrupt the ability of Rap1p to bind the telomere, increasing telomere accessibility. Although we did not extensively analyze nucleotide usage by the mutant complex, there is no detectable synthesis past the +7 position in our primer extension analyses, even in the presence of all four nucleotides, and no change in the electrophoretic mobility of the products, a characteristic that is sensitive to base sequence (49). Furthermore, addition of labeled dTTP alone to the telomerase assay results in the addition of a single nucleotide by both mutant and wild-type telomerase, suggesting that fidelity

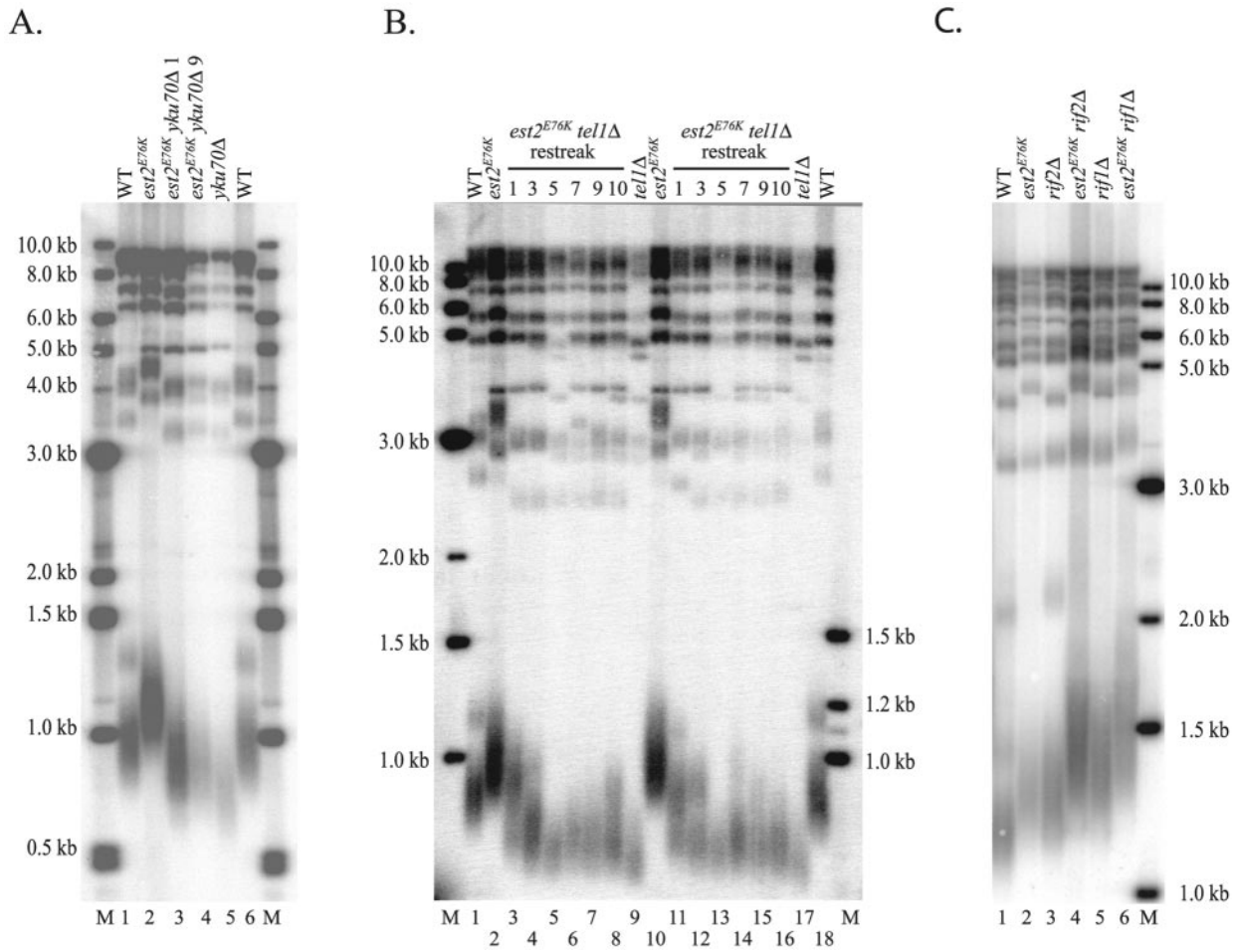

FIG. 7. Increased telomere length of the *est2*^{LT} alleles is dependent on *TEL1* but independent of *YKU70*, *RIF1*, and *RIF2*. (A) Epistasis analysis of *yku70*Δ and *est2*^{E76K}. Gene replacement was used to generate strains with *YKU70* (*yku70*::*KAN*) deleted and expressing either wild-type (WT) *EST2* (YKF203; lane 5) or *est2*^{E76K} (YKF203-E76K; lanes 3 and 4) from the endogenous, chromosomal locus. After isolation of the appropriate *yku70* disruption, the *est2*^{E76K} yku70::*KAN* strain was restreaked nine times to confirm that telomere length had stabilized. DNA isolated after restreak 1 (lane 3) and restreak 9 (lane 4) is shown. Telomere length was visualized by Southern blotting of PstI-digested genomic DNA with a telomeric probe. DNA isolated from isogenic *YKU70* strains expressing wild-type *EST2* (YKF201, lanes 1 and 6) or *est2*^{E76K} (YKF201-E76K, lane 2) was included for comparison. The positions of molecular weight markers are indicated (M). (B) Epistasis analysis of *tel1*Δ and *est2*^{E76K}. Gene replacement was used to generate strains with *tel1* deleted (*tel1*::*KAN*) and expressing either wild-type *EST2* (YKF202; lanes 9 and 17) or *est2*^{E76K} (YKF202-E76K; lanes 3 to 8 and lanes 11 to 16) from the endogenous, chromosomal locus. Because the telomere length phenotype of *tel1*Δ takes many generations to reach maximum expression, newly transformed strains were sequentially restreaked on plates. For the double mutant, two independent transformants were restreaked and DNA was prepared from restreaks 1, 3, 5, 7, 9, and 10 as indicated. Only restreak 10 of the *tel1*Δ strain is shown. Genomic DNA was digested with PstI, and telomere length was measured by Southern blotting. DNA isolated from isogenic *TEL1* strains expressing wild-type *EST2* (YKF201, lanes 1 and 18) or *est2*^{E76K} (YKF201-E76K, lanes 3 and 10) was included for comparison. The positions of molecular weight markers are indicated (M). (C) Epistasis analysis of *rif1*Δ and *rif2*Δ with *est2*^{E76K}. Gene replacement was used to generate strains with *rif2* deleted (*rif2*::*KAN*) and expressing either wild-type *EST2* (YKF205; lane 3) or *est2*^{E76K} (YKF205-E76K; lane 4) from the endogenous, chromosomal locus. Strains with *rif1* deleted (*rif1*::*KAN*) and expressing wild-type *EST2* (YKF204; lane 5) or *est2*^{E76K} (YKF204-E76K; lane 6) from the chromosomal locus were also created. Genomic DNA was digested with XhoI, and telomere length was measured by Southern blotting. DNA isolated from isogenic *RIF1* and *RIF2* strains expressing wild-type *EST2* (YKF201, lane 1) or *est2*^{E76K} (YKF201-E76K, lane 2) was included for comparison. The positions of molecular weight markers are indicated (M).

at the second template position remains high. Consistent with these observations, *est2*^{E76K} causes additional telomere lengthening in *rif1*Δ and *rif2*Δ strains, implying that telomere overelongation is independent of the *RAP1* genetic pathway.

Est2p can be physically cross-linked to oligonucleotide primer, and some mutations and deletions within the N terminus alter primer usage in a manner consistent with loss of the telomerase anchor site (32). Unlike the *est2*^{LT} alleles, these mutations cause telomere shortening, suggesting that the *est2*^{LT} phenotype does not result from loss of anchor site function. Consistent with this assertion, a primer challenge assay shows no evidence of decreased primer association by telomerase in an *est2*^{LT} strain. Telomere lengthening might occur if the enzyme-DNA interaction were increased, a possibility consistent with the semidominant nature of the *est2*^{E76K} allele. However, the amount of activity displayed by wild-type and *est2*^{E76K} telomerase on decreasing concentrations of primer is indistinguishable, indicating that the K_m for primer is not sig-

nificantly altered by the E76K mutation. We conclude that increased anchor site interaction is unlikely to account for the long-telomere phenotype, although we cannot rule out the possibility that slight differences in primer association translate into measurable changes in telomere length in vivo.

Our experiments show a slight (<2-fold) but reproducible increase in the amount of *est2*^{E76K} mutant protein that can be immunoprecipitated from cells (Fig. 1D). Interestingly, detection of wild-type and mutant ProA-Est2p in extract demonstrates equivalent expression, suggesting that the accessibility of the protein A epitope tag may be altered by the E76K mutation in Est2p. Because expression of the ProA-Est2^{E76K} protein appears unchanged, it is unlikely that differences in protein expression account for the telomere-lengthening phenotype.

PinXIp has been shown to compete with the telomerase RNA for Est2p binding (29). Therefore, decreased interaction with PinXI might increase telomere length by increasing the amount of assembled holoenzyme in vivo. Consistent with the observation that region I is not required for interaction with PinXIp (29), the ability of PinXIp to bind Est2p is not altered by the E76K mutation (Fig. S1 in the supplemental material). Indeed, although cooverexpression of Est2p and *TLC1* RNA greatly increases the amount of telomerase activity in cell extract, such overexpression does not cause telomere lengthening, presumably because other critical components of the complex or telomeric chromatin are limiting (53). Together with the observation that the interaction of Est2p with Est1p and Est3p is not altered by the E76K mutation (see Fig. S1 in the supplemental material), these data argue that the long-telomere phenotype is not due to alterations in the amount or stoichiometry of the telomerase complex.

Genetic pathway of telomere lengthening by *est2*^{LT} alleles. Given the lack of evidence for altered catalytic activity of the *est2*^{E76K} enzyme, we favor the hypothesis that these particular mutations in the N terminus of Est2p impact a regulatory pathway in vivo. This possibility is supported by the observation that deletion of the yeast ATM homolog *TEL1* is epistatic to the *est2*^{LT} mutants. Deletion of *TEL1* in the *est2*^{E76K} background almost completely abrogates the telomere-lengthening phenotype. This effect takes five restreaks (approximately 125 generations) for full expression and suggests that telomerase requires function of the Tel1 protein in order to manifest the *est2*^{LT} phenotype. This genetic result distinguishes the *est2*^{LT} alleles from mutations in *ELG1* (52) and *POL12* (20) that also cause telomere lengthening but are independent of *TEL1*.

Tel1p is hypothesized to facilitate the recruitment of telomerase to the telomere in vivo by facilitating the interaction between telomerase and its substrate, perhaps through modulating activity of the Mre11/Rad50/Xrs2 (MRX) complex (6, 46, 55). The *est2*^{LT} alleles may increase the sensitivity of telomerase to this recruitment function. Because we do not detect changes in the interaction between partially purified mutant telomerase and an oligonucleotide primer in vitro, we favor the hypothesis that such increased recruitment occurs through changes in the interaction between telomerase and components of telomeric chromatin. Although *RIF1* and *RIF2* function upstream of *TEL1*, these genes do not appear to play a role in telomere lengthening mediated by the *est2*^{LT} alleles since telomere lengthening is still apparent in strains completely lacking either *RIF1* or *RIF2*.

Interestingly, in two independent *est2*^{E76K} *tel1*Δ transformants (and in *est2*^{N95A} *tel1*Δ strains [data not shown]), we observed increased heterogeneity of the telomeric repeats at long generation times, though the minimal telomere length remained approximately the same. This phenomenon suggests that the *est2*^{LT} alleles can cause telomere lengthening through an alternative pathway that is either selected after long-term growth or becomes activated when telomere length is sufficiently short. This alternate pathway may account for the slight (~30 bp) *TEL1*-independent increase in telomere length seen at moderate generation times.

Because only a small fraction of yeast telomeres are subject to the activity of telomerase in a given cell cycle (54), we suggest that the *est2*^{LT} alleles alter either the frequency with which telomerase engages the telomere or the extent of polymerization once a telomere has been "chosen" for elongation. The increased telomere length heterogeneity of a diploid strain expressing both wild-type and mutant telomerase presumably reflects competition for telomere access between telomerase complexes that are correctly regulated and those that are at least partially refractory to that regulation. Future experiments to distinguish these possibilities may clarify the mechanism through which the *est2*^{LT} alleles cause telomere lengthening and uncover a novel role of the telomerase enzyme in telomere length regulation.

ACKNOWLEDGMENTS

We thank T. Formosa, N. Lue, V. Lundblad, and R. Wellinger for generous gifts of protocols and reagents; Y. Liu, T. Cech, and E. Fanning for critical reading of the manuscript; and T. Graham and colleagues for helpful suggestions and reagents. J. Warner, J. Lane, G. Todd, J. Smith, L. Miyatake, and E. Hysinger contributed to the mutant screen. We thank J. Brown for technical assistance.

This work was supported by Research Scholar Grant RSG-04-048-01-GMC from the American Cancer Society to K.L.F. and grant #52003905 of the Howard Hughes Medical Institute Professors Program.

REFERENCES

1. **Armbruster, B. N., S. S. Banik, C. Guo, A. C. Smith, and C. M. Counter.** 2001. N-terminal domains of the human telomerase catalytic subunit required for enzyme activity in vivo. Mol. Cell. Biol. **21:**7775–7786.
2. **Armbruster, B. N., K. T. Etheridge, D. Broccoli, and C. M. Counter.** 2003. Putative telomere-recruiting domain in the catalytic subunit of human telomerase. Mol. Cell. Biol. **23:**3237–3246.
3. **Armbruster, B. N., C. M. Linardic, T. Veldman, N. P. Bansal, D. L. Downie, and C. M. Counter.** 2004. Rescue of an hTERT mutant defective in telomere elongation by fusion with hPot1. Mol. Cell. Biol. **24:**3552–3561.
4. **Beattie, T. L., W. Zhou, M. O. Robinson, and L. Harrington.** 2000. Polymerization defects within human telomerase are distinct from telomerase RNA and TEP1 binding. Mol. Biol. Cell **11:**3329–3340.
5. **Bryan, T. M., K. J. Goodrich, and T. R. Cech.** 2000. Telomerase RNA bound by protein motifs specific to telomerase reverse transcriptase. Mol. Cell **6:**493–499.
6. **Chan, S. W. L., J. Chang, J. Prescott, and E. H. Blackburn.** 2001. Altering telomere structure allows telomerase to act in yeast lacking ATM kinases. Curr. Biol. **11:**1240–1250.
7. **Collins, K., and C. W. Greider.** 1993. *Tetrahymena* telomerase catalyzes nucleolytic cleavage and nonprocessive elongation. Genes Dev. **7:**1364–1376.
8. **Counter, C. M., A. A. Avilion, C. E. Lefeuvre, N. G. Stewart, C. W. Greider, C. B. Harley, and S. Bacchetti.** 1992. Telomere shortening associated with chromosome instability is arrested in immortal cells which express telomerase activity. EMBO J. **11:**1921–1929.
9. **Craven, R. J., and T. D. Petes.** 1999. Dependence of the regulation of telomere length on the type of subtelomeric repeat in the yeast *Saccharomyces cerevisiae*. Genetics **152:**1531–1541.
10. **Dionne, I., and R. J. Wellinger.** 1996. Cell cycle-regulated generation of

single-stranded G-rich DNA in the absence of telomerase. Proc. Natl. Acad. Sci. USA **93:**13902–13907.
11. **Formosa, T., and T. Nittis.** 1999. Dna2 mutants reveal interactions with DNA polymerase alpha and Ctf4, a Pol alpha accessory factor, and show that full Dna2 helicase activity is not essential for growth. Genetics **151:**1459–1470.
12. **Friedman, K. L., and T. R. Cech.** 1999. Essential functions of N-terminal domains in the yeast telomerase catalytic subunit revealed by selection for viable mutants. Genes Dev. **13:**2863–2874.
13. **Friedman, K. L., J. J. Heit, D. Long, and T. R. Cech.** 2003. N-terminal domain of yeast telomerase reverse transcriptase: recruitment of Est3p to the telomerase complex. Mol. Biol. Cell **14:**1–13.
14. **Fromant, M., S. Blanquet, and P. Plateau.** 1995. Direct random mutagenesis of gene-sized DNA fragments using polymerase chain reaction. Anal. Biochem. **224:**347–353.
15. **Giaever, G., A. M. Chu, L. Ni, C. Connelly, L. Riles, S. Veronneau, S. Dow, A. Lucau-Danila, K. Anderson, B. Andre, A. P. Arkin, A. Astromoff, M. El Bakkoury, R. Bangham, R. Benito, S. Brachat, S. Campanaro, M. Curtiss, K. Davis, A. Deutschbauer, K.-D. Entian, P. Flaherty, F. Foury, D. J. Garfinkel, M. Gerstein, D. Gotte, U. Guldener, J. H. Hegemann, S. Hempel, Z. Herman, D. F. Jaramillo, D. E. Kelly, S. L. Kelly, P. Kotter, D. Labonte, D. C. Lamb, N. Lan, H. Liang, H. Liao, L. Liu, C. Luo, M. Lussier, R. Mao, P. Menard, S. L. Ooi, J. L. Revuelta, C. J. Roberts, M. Rose, P. Ross-Macdonald, B. Scherens, G. Schimmack, B. Shafer, D. D. Shoemaker, S. Sookhai-Mahadeo, R. K. Storms, J. N. Strathern, G. Valle, M. Voet, G. Volckaert, C.-Y. Wang, T. R. Ward, J. Wilhelmy, E. A. Winzeler, Y. Yang, G. Yen, E. Youngman, K. Yu, H. Bussey, J. D. Boeke, M. Snyder, P. Philippsen, R. W. Davis, and M. Johnston.** 2002. Functional profiling of the *Saccharomyces cerevisiae* genome. Nature **418:**387–391.
16. **Graham, T., M. Seeger, G. Payne, V. Mackay, and S. Emr.** 1994. Clathrin-dependent localization of alpha 1,3 mannosyltransferase to the Golgi complex of *Saccharomyces cerevisiae*. J. Cell Biol. **127:**667–678.
17. **Gravel, S., M. Larrivee, P. Labrecque, and R. J. Wellinger.** 1998. Yeast Ku as a regulator of chromosomal DNA end structure. Science **280:**741–744.
18. **Greider, C. W., and E. H. Blackburn.** 1987. The telomere terminal transferase of *Tetrahymena* is a ribonucleoprotein enzyme with two kinds of primer specificity. Cell **51:**887–898.
19. **Greider, C. W., and E. H. Blackburn.** 1989. A telomeric sequence in the RNA of *Tetrahymena* telomerase required for telomere repeat synthesis. Nature **337:**331–337.
20. **Grossi, S., A. Puglisi, P. V. Dmitriev, M. Lopes, and D. Shore.** 2004. Pol12, the B subunit of DNA polymerase alpha, functions in both telomere capping and length regulation. Genes Dev. **18:**992–1006.
21. **Hammond, P. W., T. N. Lively, and T. R. Cech.** 1997. The anchor site of telomerase from *Euplotes aediculatus* revealed by photo-cross-linking to single- and double-stranded DNA primers. Mol. Cell. Biol. **17:**296–308.
22. **Hardy, C. F. J., L. Sussel, and D. Shore.** 1992. A *RAP1*-interacting protein involved in transcriptional silencing and telomere length regulation. Genes Dev. **6:**801–814.
23. **Kyrion, G., K. A. Boakye, and A. J. Lustig.** 1992. C-terminal truncation of *RAP1* results in the deregulation of telomere size, stability, and function in *Saccharomyces cerevisiae*. Mol. Cell. Biol. **12:**5159–5173.
24. **Lai, C. K., J. R. Mitchell, and K. Collins.** 2001. RNA binding domain of telomerase reverse transcriptase. Mol. Cell. Biol. **21:**990–1000.
25. **Lee, M. S., and E. H. Blackburn.** 1993. Sequence-specific DNA primer effects on telomerase polymerization activity. Mol. Cell. Biol. **13:**6586–6599.
26. **Lee, S. R., J. M. Y. Wong, and K. Collins.** 2003. Human telomerase reverse transcriptase motifs required for elongation of a telomeric substrate. J. Biol. Chem. **278:**52531–52536.
27. **Lendvay, T. S., D. K. Morris, J. Sah, B. Balasubramanian, and V. Lundblad.** 1996. Senescence mutants of *Saccharomyces cerevisiae* with a defect in telomere replication identify three additional *EST* genes. Genetics **144:**1399–1412.
28. **Levy, D. L., and E. H. Blackburn.** 2004. Counting of Rif1p and Rif2p on *Saccharomyces cerevisiae* telomeres regulates telomere length. Mol. Cell. Biol. **24:**10857–10867.
29. **Lin, J., and E. H. Blackburn.** 2004. Nucleolar protein PinX1p regulates telomerase by sequestering its protein catalytic subunit in an inactive complex lacking telomerase RNA. Genes Dev. **18:**387–396.
30. **Lingner, J., T. R. Cech, T. R. Hughes, and V. Lundblad.** 1997. Three Ever Shorter Telomere (*EST*) genes are dispensable for in vitro yeast telomerase activity. Proc. Natl. Acad. Sci. USA **94:**11190–11195.
31. **Lingner, J., T. R. Hughes, A. Shevchenko, M. Mann, V. Lundblad, and T. R. Cech.** 1997. Reverse transcriptase motifs in the catalytic subunit of telomerase. Science **276:**561–567.
32. **Lue, N. F.** 2005. A physical and functional constituent of telomerase anchor site. J. Biol. Chem. **280:**26586–26591.
33. **Lundblad, V., and E. H. Blackburn.** 1993. An alternative pathway for yeast telomere maintenance rescues est1$^-$ senescence. Cell **73:**347–360.
34. **Lundblad, V., and J. W. Szostak.** 1989. A mutant with a defect in telomere elongation leads to senescence in yeast. Cell **57:**633–643.
35. **Lustig, A. J., and T. D. Petes.** 1986. Identification of yeast mutants with altered telomere structure. Proc. Natl. Acad. Sci. USA **83:**1398–1402.
36. **Malik, H. S., W. D. Burke, and T. H. Eickbush.** 2000. Putative telomerase catalytic subunits from *Giardia lamblia* and *Caenorhabditis elegans*. Gene **251:**101–108.
37. **Marcand, S., E. Gilson, and D. Shore.** 1997. A protein-counting mechanism for telomere length regulation in yeast. Science **275:**986–990.
38. **Miller, M. C., J. K. Liu, and K. Collins.** 2000. Template definition by *Tetrahymena* telomerase reverse transcriptase. EMBO J. **19:**4412–4422.
39. **Moriarty, T. J., S. Huard, S. Dupuis, and C. Autexier.** 2002. Functional multimerization of human telomerase requires an RNA interaction domain in the N terminus of the catalytic subunit. Mol. Cell. Biol. **22:**1253–1265.
40. **Moriarty, T. J., D. T. Marie-Egyptienne, and C. Autexier.** 2004. Functional organization of repeat addition processivity and DNA synthesis determinants in the human telomerase multimer. Mol. Cell. Biol. **24:**3720–3733.
41. **Nugent, C. I., T. R. Hughes, N. F. Lue, and V. Lundblad.** 1996. Cdc13p: A single-strand telomeric DNA binding protein with a dual role in yeast telomere maintenance. Science **274:**249–252.
42. **Peng, Y., I. S. Mian, and N. F. Lue.** 2001. Analysis of telomerase processivity: mechanistic similarity to HIV-1 reverse transcriptase and role in telomere maintenance. Mol. Cell **7:**1201–1211.
43. **Porter, S., P. Greenwell, K. Ritchie, and T. Petes.** 1996. The DNA-binding protein Hdf1p (a putative Ku homologue) is required for maintaining normal telomere length in *Saccharomyces cerevisiae*. Nucleic Acids Res. **24:**582–585.
44. **Prescott, J., and E. H. Blackburn.** 1997. Functionally interacting telomerase RNAs in the yeast telomerase complex. Genes Dev. **11:**2790–2800.
45. **Ray, A., and K. W. Runge.** 1999. Varying the number of telomere-bound proteins does not alter telomere length in tel1 delta cells. Proc. Natl. Acad. Sci. USA **96:**15044–15049.
46. **Ritchie, K. B., and T. D. Petes.** 2000. The Mre11p/Rad50p/Xrs2p complex and the Tel1p function in a single pathway for telomere maintenance in yeast. Genetics **155:**475–479.
47. **Rose, M. D., F. Winston, and P. Hieter.** 1990. Methods in yeast genetics: a laboratory course manual. Cold Spring Harbor Laboratory Press, Cold Spring Harbor, N.Y.
48. **Scherer, S., and R. W. David.** 1979. Replacement of chromosome segments with altered DNA sequences constructed in vitro. Proc. Natl. Acad. Sci. USA **76:**4951–4955.
49. **Seto, A. G., K. Umansky, Y. Tzfati, A. J. Zaug, E. H. Blackburn, and T. R. Cech.** 2003. A template-proximal RNA paired element contributes to *Saccharomyces cerevisiae* telomerase activity. RNA **9:**1323–1332.
50. **Singer, M. S., and D. E. Gottschling.** 1994. *TLC1*: template RNA component of *Saccharomyces cerevisiae* telomerase. Science **266:**404–409.
51. **Smogorzewska, A., and T. De Lange.** 2004. Regulation of telomerase by telomeric proteins. Ann. Rev. Biochem. **73:**177–208.
52. **Smolikov, S., Y. Mazor, and A. Krauskopf.** 2004. *ELG1*, a regulator of genome stability, has a role in telomere length regulation and in silencing. Proc. Natl. Acad. Sci. USA **101:**1656–1661.
53. **Teixeira, M. T., K. Foerstemann, S. M. Gasser, and J. Lingner.** 2002. Intracellular trafficking of yeast telomerase components. EMBO Rep. **3:**652–659.
54. **Teixeira, M. T., M. Americ, P. Sperisen, and J. Lingner.** 2004. Telomere length homeostasis is achieved via a switch between telomerase-extendible and -nonextendible states. Cell **117:**323–335.
55. **Tsukamoto, Y., A. K. P. Taggart, and V. A. Zakian.** 2001. The role of the Mre11-Rad50-Xrs2 complex in telomerase-mediated lengthening of *Saccharomyces cerevisiae* telomeres. Curr. Biol. **11:**1328–1335.
56. **Wellinger, R. J., and D. Sen.** 1997. The DNA structures at the ends of eukaryotic chromosomes. Eur. J. Cancer **33:**735–749.
57. **Wellinger, R. J., A. J. Wolf, and V. A. Zakian.** 1993. *Saccharomyces* telomeres acquire single-strand TG1-3 tails late in S phase. Cell **72:**51–60.
58. **Wotton, D., and D. Shore.** 1997. A novel Rap1p-interacting factor, Rif2p, cooperates with Rif1p to regulate telomere length in *Saccharomyces cerevisiae*. Genes Dev. **11:**748–760.
59. **Xia, J., Y. Peng, I. S. Mian, and N. F. Lue.** 2000. Identification of functionally important domains in the N-terminal region of telomerase reverse transcriptase. Mol. Cell. Biol. **20:**5196–5207.
60. **Zakian, V. A.** 1996. Telomere functions: lessons from yeast. Trends Cell Biol. **6:**29–33.